

# Restoration of auditory evoked responses by human ES-cell-derived otic progenitors

Wei Chen<sup>1,2\*</sup>, Nopporn Jongkamonwiwat<sup>1,2,3\*</sup>, Leila Abbas<sup>1,2</sup>, Sarah Jacob Eshtan<sup>1,2</sup>, Stuart L. Johnson<sup>2</sup>, Stephanie Kuhn<sup>2</sup>, Marta Milo<sup>2</sup>, Johanna K. Thurlow<sup>1,2</sup>, Peter W. Andrews<sup>1,2</sup>, Walter Marcotti<sup>2</sup>, Harry D. Moore<sup>1,2</sup> & Marcelo N. Rivolta<sup>1,2</sup>

**Deafness is a condition with a high prevalence worldwide, produced primarily by the loss of the sensory hair cells and their associated spiral ganglion neurons (SGNs). Of all the forms of deafness, auditory neuropathy is of particular concern. This condition, defined primarily by damage to the SGNs with relative preservation of the hair cells<sup>1</sup>, is responsible for a substantial proportion of patients with hearing impairment<sup>2</sup>. Although the loss of hair cells can be circumvented partially by a cochlear implant, no routine treatment is available for sensory neuron loss, as poor innervation limits the prospective performance of an implant<sup>3</sup>. Using stem cells to recover the damaged sensory circuitry is a potential therapeutic strategy. Here we present a protocol to induce differentiation from human embryonic stem cells (hESCs) using signals involved in the initial specification of the otic placode. We obtained two types of otic progenitors able to differentiate *in vitro* into hair-cell-like cells and auditory neurons that display expected electrophysiological properties. Moreover, when transplanted into an auditory neuropathy model, otic neuroprogenitors engraft, differentiate and significantly improve auditory-evoked response thresholds. These results should stimulate further research into the development of a cell-based therapy for deafness.**

Hair-cell-like phenotypes and sensory neurons, with different degrees of functional maturation, have been obtained from mouse stem populations<sup>4–10</sup>. After transplantation, some cell types have shown engraftment but none have shown evidence of functional recovery<sup>10–15</sup>. Although useful for research purposes, these products are unsuitable for a therapeutic application and appropriate cell types of human origin have remained elusive so far. Neuroprogenitors isolated from mature human cochleae display limited proliferative and differentiating potential<sup>16</sup>, hESC-derived neural crest cells may differentiate into sensory neurons by exposure to bone morphogenetic protein (BMP) but lack true otic characteristics<sup>17,18</sup>. Recently, we isolated a population of bipotent stem cells from the human fetal cochlea (human fetal auditory stem cells, hFASCs), with the ability to produce hair-cell-like cells and neurons<sup>19</sup>. However, although hFASCs can be expanded *in vitro* for approximately 25 population doublings, they eventually undergo replicative senescence. Hence, there is a need for a reliable, renewable source of human otic progenitors, with the ability to produce both cell types for sensory replacement.

Fibroblast growth factor (FGF) signalling is necessary and sufficient for the induction *in vivo* of the otic placode, the primordium of the hearing organ<sup>20,21</sup>. As the ligands involved in placode signalling in the mouse have been identified as FGF3 and FGF10 (refs 22, 23), we proposed that exposure to these factors would trigger otic differentiation of hESCs. Initial experiments with embryoid bodies confirmed FGF3 and FGF10 induction of otic features (Supplementary Fig. 1a). We therefore focused on developing a method devoid of this initial cell-aggregation step, which is prone to high variability. Undifferentiated colonies of hESCs were dissociated for plating as a monolayer on

laminin-coated flasks (see Supplementary Methods). Under these conditions, treatment with FGF3 and FGF10 induced the placodal markers PAX8 and PAX2, either in the presence of knockout serum replacement or under defined conditions using Dulbecco's Modified Eagle's Medium (DMEM) with Ham's F12 and N2/B27 (DFNB) medium (Supplementary Methods and Supplementary Figs 1b and 2). Global analyses of gene expression was performed using Affymetrix GeneChip arrays and, after normalization (see Supplementary Methods), samples were mined in two different ways. We first used the Gene Set Enrichment Analysis (GSEA) tool<sup>24</sup> to look for genes that were enriched in the entire list of probe sets, without establishing a priori cut off of differential expression (Supplementary Tables 1 and 2). This analysis showed that a set of otic markers was significantly enriched in the FGF-treated samples when compared with the undifferentiated hESCs (normalized enriched score (NES), 0.568; family-wise error rate (FWER)  $P = 0.046$ ) or cells grown in DFNB (NES, 0.707; FWER  $P = 0.019$ ) (Supplementary Table 1). A second type of analysis assessed genes differentially expressed using predefined criteria for fold-change cut off and statistical significance (see Supplementary Methods). A total of 1,424 genes (represented by 2,124 probe sets) was differentially upregulated in the FGF samples when compared to undifferentiated hESCs, whereas 423 genes (505 probe sets) were unregulated in the FGF-treated versus the DFNB controls (Supplementary Tables 3 and 4). Conversely, 2,368 genes (3,231 probe sets) were downregulated in the FGF samples versus hESCs, and 482 genes (607 probe sets) were downregulated versus DFNB (Supplementary Tables 5 and 6). In a gene ontology analysis, the gene ontology terms 'sensory organ development' (Expression Analysis Systematic Explorer (EASE)  $P$  value score in FGF versus hESC,  $P = 3.92 \times 10^{-15}$ ; FGF versus DFNB,  $P = 0.022$ ); 'ear development' (FGF versus hESC,  $P = 4.47 \times 10^{-8}$ ; FGF versus DFNB,  $P = 0.014$ ) and 'ear morphogenesis' (FGF versus hESC,  $P = 3.08 \times 10^{-6}$ ; FGF versus DFNB,  $P = 0.0497$ ) were highly enriched in the FGF-treated cells in both comparisons, and 'mechanoreceptor differentiation' and 'auditory receptor differentiation' were highly enriched in FGF versus hESC (see Supplementary Tables 7–10). Both bioinformatics analyses therefore suggested that the FGF treatment was generating a global change of transcription compatible with the induction of otic progenitors.

We also used immunostaining to examine the co-expression of PAX8 and SOX2, to define the otic progenitors at a cellular level. Otic progenitors grew as colonies after the inductive phase. Initial immunolabelling showed a relatively large proportion of double-positive cells in the FGF-treated condition (~78%), in contrast to the relatively moderate upregulation of otic transcripts detected with the arrays. However, a subset of cells expressed very high levels of PAX8 and SOX2, and these were assessed with an automated microscopy platform (InCell Analyzer 1000) that enabled quantification of the number of positive cells and their relative intensity (Fig. 1 and Supplementary Fig. 3). When a stringent threshold was selected

<sup>1</sup>Centre for Stem Cell Biology, University of Sheffield, Sheffield S10 2TN, UK. <sup>2</sup>Department of Biomedical Sciences, University of Sheffield, Sheffield S10 2TN, UK. <sup>3</sup>Faculty of Health Sciences, Srinakharinwirot University, Ongkharak, Nakhonnayok 26120, Thailand.

\*These authors contributed equally to this work.

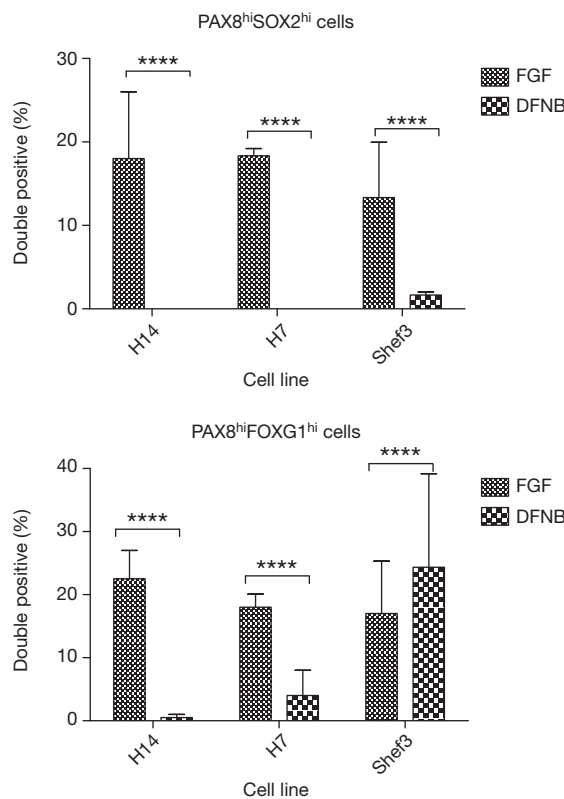


**Figure 1 | FGF3 and FGF10 generate otic progenitors.** Bar charts showing the percentage of PAX8<sup>hi</sup>SOX2<sup>hi</sup>-expressing (top panel) and PAX8<sup>hi</sup>FOXG1<sup>hi</sup>-expressing (bottom panel) cells at the FGF 75th percentile threshold, obtained from the hESC lines H14, H7 and Shef3 ( $n = 3$ ). Error bars, mean + s.e.m.

(75th intensity percentile per cell line and antibody; see Supplementary Methods)  $18.3\% \pm 0.8$  ( $\pm$  s.e.m.) of the cells expressed high levels of PAX8 and SOX2 (PAX8<sup>hi</sup>SOX2<sup>hi</sup>) after FGF treatment (against 0% obtained without the growth factors,  $P < 0.001$ ), whereas  $18\% \pm 2$  cells were PAX8<sup>hi</sup>FOXG1<sup>hi</sup> (compared to  $4\% \pm 4$  cells for the control,  $P < 0.001$ ). PAX8<sup>hi</sup>SOX2<sup>hi</sup>FOXG1<sup>hi</sup> cells also expressed the otic markers PAX2, nestin, SIX1 and GATA3 (Fig. 2h and Supplementary Figs 4 and 5a). It is likely that this subset of PAX8<sup>hi</sup>SOX2<sup>hi</sup>FOXG1<sup>hi</sup>-expressing cells represents the otic progenitors. The reproducibility of the protocol was tested across the hESC lines H7, H14 and Shef3, which all gave comparable results (see Fig. 1 and Supplementary Fig. 3). FGF3 and FGF10 induced two morphologically distinct types of otic colonies (Fig. 2a–h). One cell population showed a flat phenotype, with large cytoplasm and formed epithelioid islands (Fig. 2a–d), whereas the second was small, with denser chromatin, and presented cytoplasmic projections (Fig. 2e, f). Given their morphological appearance, we have operationally named them otic epithelial progenitors (OEPs) and otic neural progenitors (ONPs), respectively. The relative proportion of these progenitors was dependent on the cell line, plating density and the degree of cell separation (single cells versus cell clusters) (Supplementary Figs 5 and 6 and Supplementary Methods). Progenitor colonies were purified using sequential dissociation (see Supplementary Methods), yielding moderately homogenous cultures of the desired cell colony type, and were expanded in OSCFM (otic stem cell full media; see Supplementary Methods).

The differentiation potential of OEPs and ONPs was tested in ‘neuralizing’ and ‘hair-cell’ culture conditions developed previously using hFASCs<sup>19</sup> (see Supplementary Methods). OEPs produced hair-cell-like cells as defined by the simultaneous expression of ATOH1 and BRN3C, or BRN3C and MYO7A (~45%) (Supplementary Fig. 7). A small subset differentiated a rudimentary apical bundle, expressing

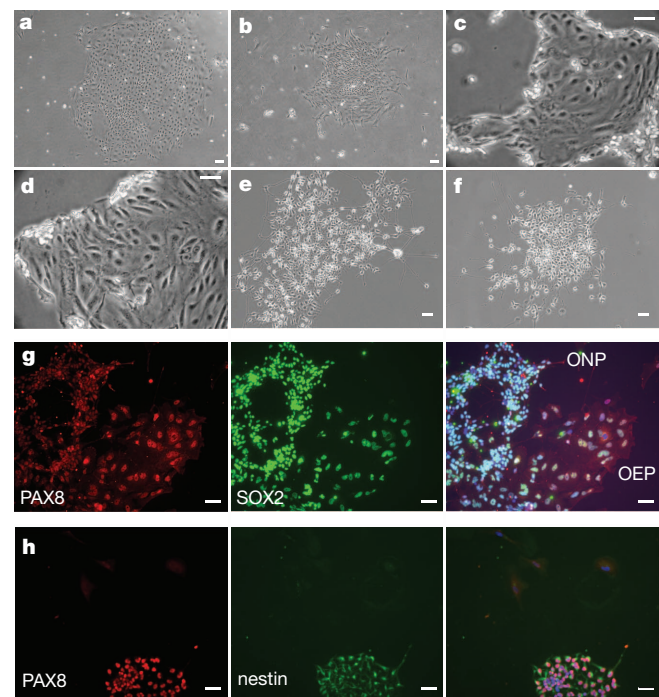


**Figure 2 | Otic epithelial progenitors and otic neuro progenitors.**

**a, b**, Morphology of an OEP colony. Scale bars, 100  $\mu$ m. **c, d**, The partial lifting of OEPs when treated with a short, mild trypsin incubation. Scale bars, 50  $\mu$ m. **e, f**, Typical morphology of ONPs, showing cytoplasmic projections. Scale bars, 50  $\mu$ m. **g**, Side-by-side ONP and OEP colonies, double-labelled for PAX8 and SOX2. Scale bars, 50  $\mu$ m. **h**, ONP colony labelled for PAX8 and nestin. Scale bars, 50  $\mu$ m.

espin (Supplementary Fig 8). These hair-cell-like cells also expressed an outward K<sup>+</sup> current, the inward rectifier K<sup>+</sup> current  $I_{K1}$  and an inward Ca<sup>2+</sup> current ( $I_{Ca}$ ) (Supplementary Fig. 9). Under neuralizing conditions, they produced a small proportion (~9%) of sensory neurons (Supplementary Fig. 7). Conversely, ONPs were committed to produce neurons. Under neuralizing conditions, almost all cells developed a bipolar morphology and were positive for BRN3A and  $\beta$ -tubulin III, as well as for  $\beta$ -tubulin III and NF200. They also expressed NEUROD1, ISL1 and NTRK2, a delayed-rectifier K<sup>+</sup> current ( $I_K$ ), an Na<sup>+</sup> current ( $I_{Na}$ ), and elicited single action potentials (Supplementary Fig. 9). No hair-cell differentiation was obtained from ONPs under neuralizing or hair-cell culture conditions. Detailed results are given in Supplementary Information.

The properties of ONPs *in vivo* were studied by transplanting them into ouabain-treated gerbils, a model of neuropathic deafness<sup>25</sup>. Application of ouabain directly to the round window selectively damages the type I SGNs, preserving the hair cells and the organ of Corti<sup>26</sup> (Supplementary Fig. 10). After ouabain application, only a small number of SGNs survived (6.4%; see Supplementary Table 11). Most of the surviving cells (~87%) were peripherin-positive type II neurons, therefore less than 1% of the original population of type I neurons remained (Supplementary Table 11 and Supplementary Fig. 13). Staining for myosin VIIa and the presence of distortion product otoacoustic emissions (DPOAEs) confirmed that the organ of Corti had not been damaged (Supplementary Figs 10 and 11). DPOAEs are sounds produced as a consequence of electromechanical feedback from the outer hair cells and can be used to check their physiological integrity.

ONPs derived from Shef1 hESCs constitutively expressing either enhanced green fluorescent protein (eGFP) or tomato fluorescent protein were expanded in OSCFM, dissociated with trypsin and delivered directly into the modiolus, approaching the cochlea through the round window. One set of animals was transplanted 3 to 5 days

after ouabain application ( $n = 13$ ), and another was transplanted 2 weeks after the ototoxic drug ( $n = 5$ ). As no functional or histological differences were encountered between the two groups ( $P > 0.05$ ; Supplementary Fig. 12), they were analysed together. Two to three weeks after transplantation, five out of six animals had surviving, transplanted cells grafted in the modiolus, forming an ectopic spiral ganglion (Fig. 3a, b). Cells in the marginal sides of the ectopic ganglion had undergone differentiation as judged by  $\beta$ -tubulin III staining (Fig. 3b) and displayed neural projections, targeting the organ of Corti (Fig. 3c, d). Animals were then monitored for 10 weeks post transplantation. Histological analysis after 10 weeks post transplantation showed that the ectopic ganglion was still present and that cells had also migrated into the Rosenthal's canal (Fig. 3e). Transplanted cells expressed the 3A10 neurofilament-associated antigen and NKA $\alpha$ 3 (ATP1A3), a marker of type I neurons and afferent fibres in

the inner ear<sup>27</sup> (Supplementary Fig. 14). Notably, projections from the transplanted cells that reached the organ of Corti were targeting the hair cells, and fibres positive for NKA $\alpha$ 3 and GluA2 were found next to the basal pole of the inner hair cells, suggesting the presence of synaptic connections (Fig. 3g). Moreover, fibres from the transplanted cells were visualized leaving the modiolus towards the brainstem (Fig. 3f). In the cochlear nucleus of three gerbils we found red fluorescent protein (RFP)-positive fibres also stained for synaptophysin, suggesting synaptic connections with the central auditory path (Fig. 3h, i). Transplanted ONPs contributed significantly to restore neuronal density (Fig. 3j;  $P < 0.01$ ). Although  $112.5 \pm 11.9$  TUJ1 $^+$  cells per mm $^2$  ( $\pm$  s.e.m.) were present in the ouabain-treated, untransplanted ears,  $546.4 \pm 30.6$  TUJ1 $^+$  cells per mm $^2$  were found after transplantation. From these,  $94.9 \pm 0.3\%$  were also GFP- (or tomato)-positive, confirming their exogenous nature (Supplementary Table 12). The number of projections detected in the brainstem was considerably lower than the number of transplanted cell bodies identified in the ganglion. Although this could be explained by the limited sorting of fluorescent protein into the long afferent fibres, the pathfinding of the central innervations requires further future exploration. No tumours were detected in any of the transplanted animals at any stage throughout the experiment.

Functional performance was determined by measuring auditory-evoked response (ABR) thresholds. These were established based on the wave ii-wave iii (P2–N3 waveform) amplitude<sup>28</sup>. These waves are generated by the cochlear nucleus and the superior olive complex cells, and reflect neural connections with the central auditory pathway<sup>29</sup>. After ouabain application, auditory function was severely impaired, with thresholds rising from 20 dB sound pressure level (SPL) to almost 80 dB SPL, the maximum intensity tested. Frequency discrimination was also abolished. The amplitudes of wave ii-wave iii complexes were almost negligible at any of the frequencies explored at the maximum intensity of 80 dB SPL (Fig. 4d). ABRs were recorded at 1- to 2-week intervals. Control animals ( $n = 8$ ) showed no sign of functional recovery throughout the experiment, with a mean auditory threshold after 10 weeks of  $75.14 \pm 2.3$  dB ( $\pm$  s.e.m.); similar to the  $76.37 \pm 1.8$  dB obtained after ouabain treatment. However, in the transplanted animals ( $n = 18$ ), there was a detectable improvement in the ABR thresholds (Fig. 4a, b) starting approximately 4 weeks post transplantation, with the

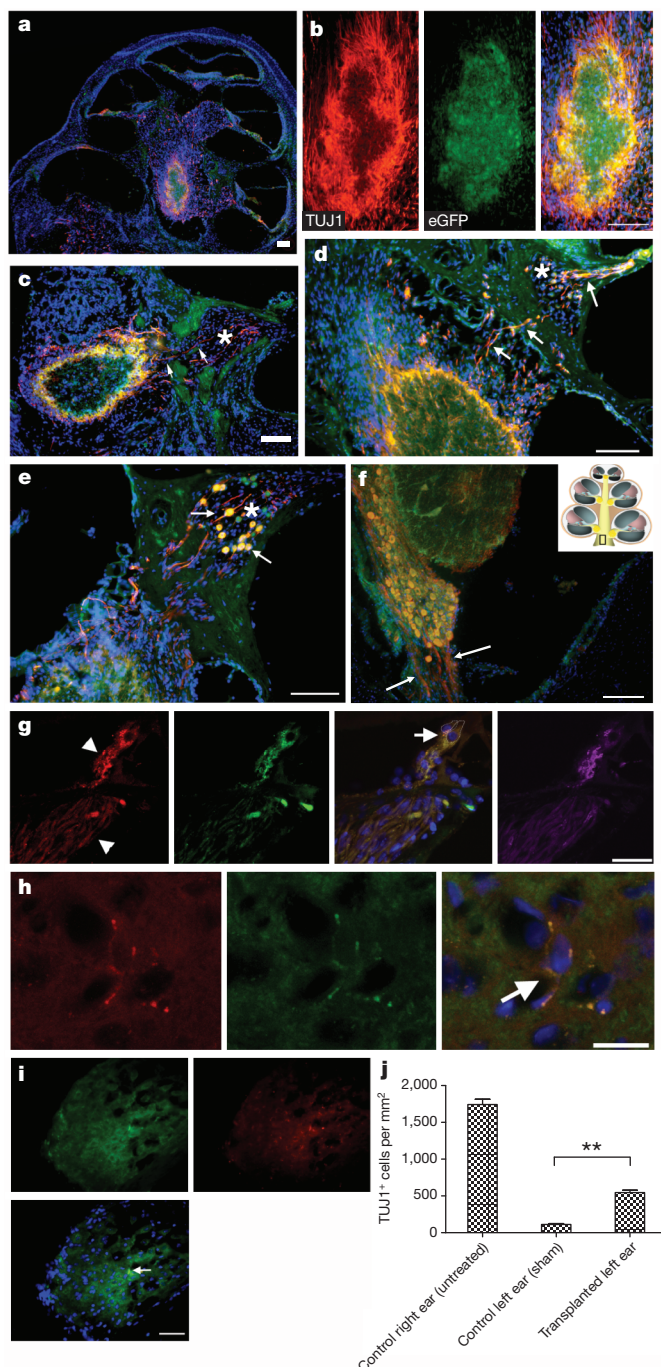


**Figure 3 | Transplantation of otic progenitors restores a population of spiral ganglion neurons.** a, Mid-modiolar section of a transplanted cochlea showing the location of the newly formed, ectopic ganglion. b, Detail of the ganglion showing neuronal differentiation by TUJ1 staining (left panel), with eGFP (middle panel) and an overlaid image (right panel). c, d, Neural fibres project from the ganglion towards the organ of Corti (arrows), passing through the Rosenthal's canal (asterisk). e, New neuronal bodies (arrows) are also found in the Rosenthal's canal (asterisk). f, Ectopic ganglion at the base of the modiolus, projecting TUJ1 $^+$  fibres centrally towards the internal auditory meatus. Inset, schematic of the cochlea showing the location of the ectopic ganglion. g, RFP $^+$  fibres (left panel; arrowheads) approaching the inner hair cells and expressing GluA2 (middle-left panel), primarily concentrated in postsynaptic densities (PSDs) around the basal pole of inner hair cells (IHCs) (middle-right panel; arrow). Dotted lines show the positions of the IHCs. Fibres (including PSDs) were also positive for NKA $\alpha$ 3 (also known as ATP1A3; right panel), a marker of afferent terminals. Nine out of ten animals analysed had fibres contacting the IHC, whereas the three animals labelled for GluA2 were positive for this marker. h, i, RFP $^+$  fibres in the cochlear nucleus, expressing synaptophysin (arrows). The fibre branches and surrounds the cell (h), with morphology highly reminiscent of the maturing endbulb of Held. Left, RFP; middle, synaptophysin; right, overlaid image. j, SGN density 10 weeks after transplantation. Conditions compared are cochleae treated with ouabain and sham-operated (control left ear (sham)) versus those treated with ouabain and transplanted with ONPs (transplanted left ear). Density was significantly increased ( $P < 0.01$ ) from  $112.5 \pm 11.9$  (control left ear (sham);  $n = 3$ ; mean  $\pm$  s.e.m.) to  $546.4 \pm 30.6$  (transplanted left ear;  $n = 8$ ). As a reference, the density of control, right ear untreated cochleae, was  $1,743 \pm 71.5$  TUJ1 $^+$  cells per mm $^2$ . \*\* $P < 0.01$ . Scale bars for a–f, 100  $\mu$ m; for g–i, 50  $\mu$ m.

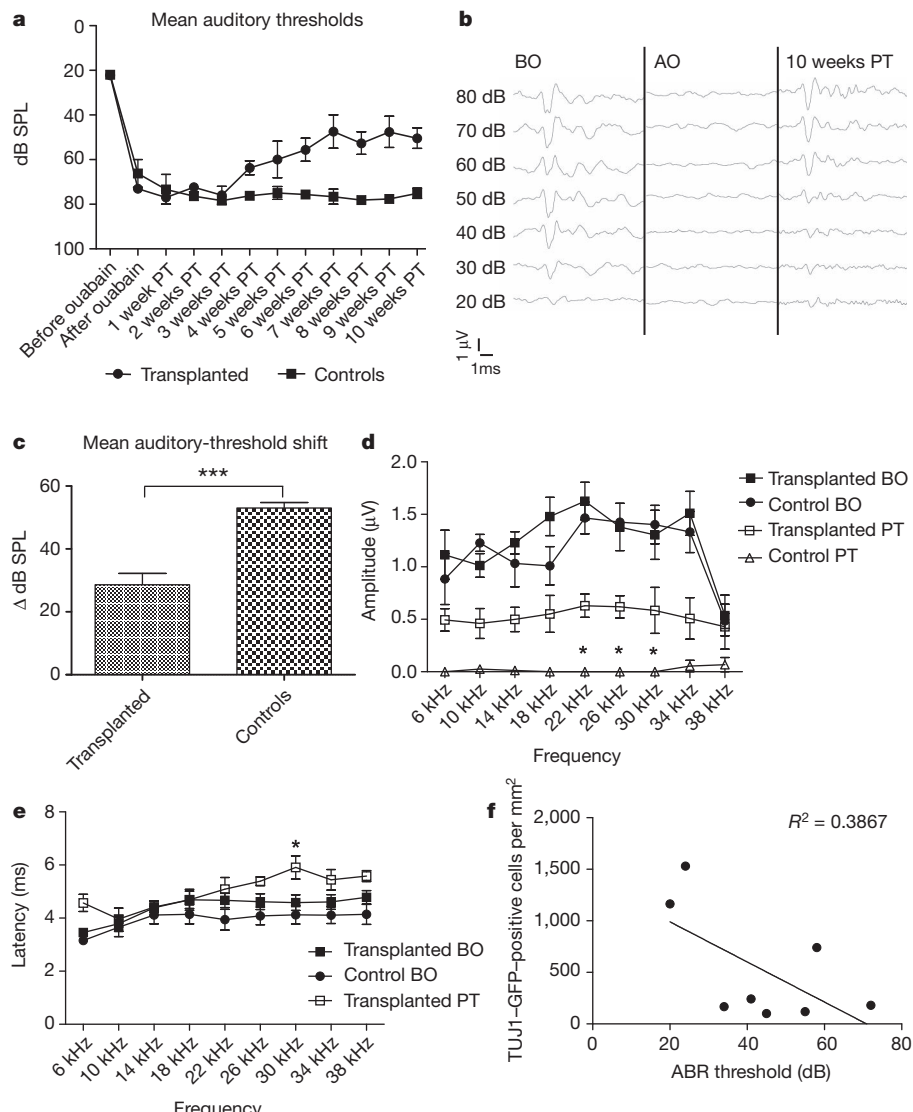


**Figure 4 | Transplanted cells provide a recovery of ABR thresholds.**

a, Evolution of the mean ABR thresholds (click) obtained in the transplanted animals ( $n = 18$ ; mean  $\pm$  s.e.m.) compared to the controls ( $n = 8$ ). b, Trace ABR showing the abolition of waves after ouabain (AO) treatment and the restoration of the complexes 10 weeks post transplantation (PT). c, Graph showing the mean auditory-threshold shift reduction obtained by the transplantation (transplanted  $28.6 \pm 3.6$  dB;  $n = 18$  versus  $53 \pm 1.7$  dB;  $n = 8$  in the control,  $P = 0.0002$ ; mean  $\pm$  s.e.m.). d, Comparison of the wave ii-wave iii amplitudes obtained by tone ABRs. A general trend of enhanced amplitudes was obtained across all frequencies tested, being significantly (\* $P < 0.05$ )

mean auditory threshold lowered (improved) to  $50.4 \pm 4.5$  dB by 10 weeks post transplantation. Furthermore, the mean auditory threshold shift, calculated as the difference between the threshold at 10 weeks post transplantation versus the one before ouabain treatment, was of  $53 \pm 1.7$  dB in the control animals, compared to  $28.6 \pm 3.6$  dB in the transplanted cohort ( $P = 0.0002$ ; Fig. 4c). This represents an overall functional improvement of approximately 46%. The range of recovery went from modest to almost complete (see Supplementary Fig. 15), which is remarkable considering the technical challenges involved in the procedure. Tonotopical processing was also partially restored (Fig. 4d). A trend in the increment of wave ii-wave iii amplitudes was detected at each frequency explored, with amplitudes being significantly different at 22, 26 and 30 kHz, when compared to the untransplanted animals ( $P < 0.05$ ). When compared to the amplitudes before the ouabain application, the improvement was approximately 43%. Latencies were mostly similar to the ones before ouabain (Fig. 4e).

different from the untransplanted controls at 22, 26 and 30 kHz. Amplitudes before ouabain were equivalent between the transplanted ( $n = 6$ ) and untransplanted animals ( $n = 5$ ; mean  $\pm$  s.e.m.). e, Latencies of wave ii-wave iii complexes were, in general, comparable before ouabain and after transplantation. Only at 30 kHz was a significant delay was observed (BO:  $4.58 \pm 0.2$  ms,  $n = 6$ ; PT:  $5.9 \pm 0.4$  ms,  $n = 5$ ;  $P < 0.05$ ; mean  $\pm$  s.e.m.). f, A significant correlation was observed between the mean density of TUJ1-GFP-positive cells and the ABR thresholds ( $n = 8$ ;  $P < 0.05$ ). \* $P < 0.05$ ; \*\*\* $P < 0.001$ .

The only significant difference was detected at 30 kHz (before ouabain,  $4.58 \pm 0.2$  ms,  $n = 6$ ; post transplantation,  $5.9 \pm 0.4$  ms,  $n = 5$ ;  $P < 0.05$ ), suggesting that some maturation was still taking place at this stage. Finally, there was a significant correlation between the increment of neural density by transplanted cells and the lowering of the ABR threshold ( $R^2 = 0.3867$ ,  $P < 0.05$ ; Fig. 4f).

Our developmentally informed protocol produced hESC-derived auditory hair cells and neurons that closely resembled phenotypes obtained from hFASCs, providing validation of their cochlear characteristics. This was supported further by the restoration of ABR thresholds on transplantation of otic progenitors into a deaf adult mammal. The ability to reinstate auditory neuron functionality paves the way for a future cell-based treatment for auditory neuropathies. It may also, in combination with a cochlear implant, offer a therapeutic solution to a wider range of patients that currently remain without viable treatment.

## METHODS SUMMARY

hESCs lines used (H7, H14, Shef1, Shef3, Shef1-eGFP and Shef1-tomato), with a normal karyotype, were maintained on mouse embryonic fibroblast feeders (MEFs) under standard conditions. Although experiments with embryoid bodies and initial monolayer experiments were carried out in the presence of KOSR, we later adopted a chemically defined medium. This serum-free, chemically defined basal culture media included a 1:1 mixture of Dulbecco's Modified Eagle's Medium (DMEM):Ham's F12 and N2/B27 supplements. In most experiments, FGF3 and FGF10 were used at 50 ng ml<sup>-1</sup>. Laminin (R&D Systems) was used at 5 µg cm<sup>-2</sup>. Antibodies, polymerase chain reaction (PCR) primers and microarray analysis are detailed in the Supplementary Methods. To induce hair-cell differentiation, progenitors were transferred to gelatin-coated dishes and cultured with DFN-B supplemented with all-*trans* retinoic acid (10<sup>-6</sup> M; Sigma) and epidermal growth factor (EGF) (20 ng ml<sup>-1</sup>) for 2 to 4 weeks. To induce neuronal differentiation, cells dissociated with trypsin were plated on gelatin-coated dishes and incubated in DFN-B with basic FGF (20 ng ml<sup>-1</sup>) and Sonic hedgehog (Shh-C24II, 500 ng ml<sup>-1</sup>; R&D Systems). On the third day, culture was supplemented with neurotrophin 3 (NTF3, 10 ng ml<sup>-1</sup>; Petropech) and brain-derived neurotrophic factor (BDNF, 10 ng ml<sup>-1</sup>; Petropech). Shh-C24II was removed on the fourth or fifth day, whereas the neurotrophins remained for the length of the incubation, normally between 7 and 14 days. Conditions for electrophysiological recordings are detailed in the Supplementary Methods. The auditory neuropathy model was generated by applying 1 mM ouabain directly into the round-window niche of adult gerbils. Either 3 days or 2 weeks later, hONPs expressing eGFP or tomato fluorescent protein, were injected into the modiolus. Functional recovery was monitored weekly by measuring ABRs and DPOAEs, for up to 10 weeks. Cochleae were taken, fixed and processed for analysis. Details of the hearing test and histological preparation are provided in the Supplementary Methods.

**Full Methods** and any associated references are available in the online version of the paper.

Received 31 July 2010; accepted 16 July 2012.

Published online 12 September 2012.

- Vlastarakos, P.V., Nikolopoulos, T.P., Tavoulari, E., Papacharalambous, G. & Korres, S. Auditory neuropathy: endocochlear lesion or temporal processing impairment? Implications for diagnosis and management. *Int. J. Pediatr. Otorhinolaryngol.* **72**, 1135–1150 (2008).
- Uus, K. & Bamford, J. Effectiveness of population-based newborn hearing screening in England: ages of interventions and profile of cases. *Pediatrics* **117**, e887–e893 (2006).
- Bradley, J., Beale, T., Graham, J. & Bell, M. Variable long-term outcomes from cochlear implantation in children with hypoplastic auditory nerves. *Cochlear Implants Int.* **9**, 34–60 (2008).
- Li, H., Liu, H. & Heller, S. Pluripotent stem cells from the adult mouse inner ear. *Nature Med.* **9**, 1293–1299 (2003).
- Li, H., Roblin, G., Liu, H. & Heller, S. Generation of hair cells by stepwise differentiation of embryonic stem cells. *Proc. Natl Acad. Sci. USA* **100**, 13495–13500 (2003).
- Oshima, K. et al. Mechanosensitive hair cell-like cells from embryonic and induced pluripotent stem cells. *Cell* **141**, 704–716 (2010).
- Jeon, S. J., Oshima, K., Heller, S. & Edge, A. S. Bone marrow mesenchymal stem cells are progenitors *in vitro* for inner ear hair cells. *Mol. Cell. Neurosci.* **34**, 59–68 (2007).
- Kondo, T., Johnson, S. A., Yoder, M. C., Romand, R. & Hashino, E. Sonic hedgehog and retinoic acid synergistically promote sensory fate specification from bone marrow-derived pluripotent stem cells. *Proc. Natl Acad. Sci. USA* **102**, 4789–4794 (2005).
- Coleman, B., Fallon, J. B., Pettingill, L. N., de Silva, M. G. & Shepherd, R. K. Auditory hair cell explant co-cultures promote the differentiation of stem cells into bipolar neurons. *Exp. Cell Res.* **313**, 232–243 (2007).
- Reyes, J. H. et al. Glutamatergic neuronal differentiation of mouse embryonic stem cells after transient expression of neurogenin 1 and treatment with BDNF and GDNF: *in vitro* and *in vivo* studies. *J. Neurosci.* **28**, 12622–12631 (2008).
- Corrales, C. E. et al. Engraftment and differentiation of embryonic stem cell-derived neural progenitor cells in the cochlear nerve trunk: growth of processes into the organ of Corti. *J. Neurobiol.* **66**, 1489–1500 (2006).
- Hildebrand, M. S. et al. Survival of partially differentiated mouse embryonic stem cells in the scala media of the guinea pig cochlea. *J. Assoc. Res. Otolaryngol.* **6**, 341–354 (2005).
- Sekiya, T. et al. Transplantation of conditionally immortal auditory neuroblasts to the auditory nerve. *Eur. J. Neurosci.* **25**, 2307–2318 (2007).
- Lang, H. et al. Transplantation of mouse embryonic stem cells into the cochlea of an auditory-neuropathy animal model: effects of timing after injury. *J. Assoc. Res. Otolaryngol.* **9**, 225–240 (2008).
- Hu, Z., Ulfendahl, M. & Olivius, N. P. Central migration of neuronal tissue and embryonic stem cells following transplantation along the adult auditory nerve. *Brain Res.* **1026**, 68–73 (2004).
- Rask-Andersen, H. et al. Regeneration of human auditory nerve. In vitro/in vivo demonstration of neural progenitor cells in adult human and guinea pig spiral ganglion. *Hear. Res.* **203**, 180–191 (2005).
- Shi, F., Corrales, C. E., Liberman, M. C. & Edge, A. S. BMP4 induction of sensory neurons from human embryonic stem cells and reinnervation of sensory epithelium. *Eur. J. Neurosci.* **26**, 3016–3023 (2007).
- Lee, G. et al. Isolation and directed differentiation of neural crest stem cells derived from human embryonic stem cells. *Nature Biotechnol.* **25**, 1468–1475 (2007).
- Chen, W. et al. Human fetal auditory stem cells can be expanded *in vitro* and differentiate into functional auditory neurons and hair cell-like cells. *Stem Cells* **27**, 1196–1204 (2009).
- Martin, K. & Groves, A. K. Competence of cranial ectoderm to respond to Fgf signaling suggests a two-step model of otic placode induction. *Development* **133**, 877–887 (2006).
- Freter, S., Muta, Y., Mak, S. S., Rinkwitz, S. & Ladher, R. K. Progressive restriction of otic fate: the role of FGF and Wnt in resolving inner ear potential. *Development* **135**, 3415–3424 (2008).
- Alvarez, Y. et al. Requirements for FGF3 and FGF10 during inner ear formation. *Development* **130**, 6329–6338 (2003).
- Wright, T. J. & Mansour, S. L. Fgf3 and Fgf10 are required for mouse otic placode induction. *Development* **130**, 3379–3390 (2003).
- Subramanian, A. et al. Gene set enrichment analysis: a knowledge-based approach for interpreting genome-wide expression profiles. *Proc. Natl Acad. Sci. USA* **102**, 15545–15550 (2005).
- Schmiedt, R. A., Okamura, H. O., Lang, H. & Schulte, B. A. Ouabain application to the round window of the gerbil cochlea: a model of auditory neuropathy and apoptosis. *J. Assoc. Res. Otolaryngol.* **3**, 223–233 (2002).
- Lang, H., Schulte, B. A. & Schmiedt, R. A. Ouabain induces apoptotic cell death in type I spiral ganglion neurons, but not type II neurons. *J. Assoc. Res. Otolaryngol.* **6**, 63–74 (2005).
- McLean, W. J., Smith, K. A., Glowatzki, E. & Pyott, S. J. Distribution of the Na,K-ATPase alpha subunit in the rat spiral ganglion and organ of corti. *J. Assoc. Res. Otolaryngol.* **10**, 37–49 (2009).
- Burkard, R., Boettcher, F., Voigt, H. & Mills, J. Comments on "Stimulus dependencies of the gerbil brain-stem auditory-evoked response (BAER). I: Effects of click level, rate and polarity" [J. Acoust. Soc. Am. 85, 2514–2525 (1989)]. *J. Acoust. Soc. Am.* **94**, 2441–2442 (1993).
- Boettcher, F. A., Mills, J. H. & Norton, B. L. Age-related changes in auditory evoked potentials of gerbils. I. Response amplitudes. *Hear. Res.* **71**, 137–145 (1993).

**Supplementary Information** is available in the online version of the paper.

**Acknowledgements** This work was supported primarily by grants from Action on Hearing Loss (RNID) to M.N.R. Other support included Deafness Research UK (M.N.R. and W.M.), the Wellcome Trust (088719, W.M.), Medical Research Council (P.W.A., H.D.M. and M.N.R.) and ESTOOLS (P.W.A.). S.L.J. was supported by a Wellcome Trust VIF award and the RNID. W.M. and S.L.J. are Royal Society university research fellows. Confocal images were taken at the Light Microscopy Facility of the Department of Biomedical Sciences, University of Sheffield. We are grateful for the advice of M. Mulheran and I. Russell on the tests of auditory function, provided at the earlier stages of this project, and to the assistance of P. Gokhale on the use of the InCell Analyzer. M.N.R. acknowledges the support and encouragement of his late parents, Noemí Luján-Ceballos and Juan Carlos Rivolta.

**Author Contributions** W.C., N.J., L.A., S.J.E and J.K.T. collected and/or assembled, analysed and interpreted data. S.L.J., S.K. and W.M. collected and/or assembled, analysed and interpreted electrophysiology data. M.M. carried out biocomputational analysis of gene-array data. P.W.A. and H.D.M. provided study material and administrative support. M.N.R. was responsible for conceiving and designing the study, for obtaining financial support, collecting and/or assembling, analysing and interpreting data, for manuscript writing, and for final approval of the manuscript.

**Author Information** Microarray datasets have been deposited at the NCBI Gene Expression Omnibus and they can be retrieved with accession number GSE36754. Reprints and permissions information is available at [www.nature.com/reprints](http://www.nature.com/reprints). The authors declare no competing financial interests. Readers are welcome to comment on the online version of the paper. Correspondence and requests for materials should be addressed to M.N.R. (m.n.rivolta@sheffield.ac.uk).

## METHODS

**Human ES-cell culture.** hESC lines H7, H14, Shef1 (including the derivatives Shef1-GFP and Shef1-tomato) and Shef3 with a normal karyotype were maintained on inactivated mouse embryonic fibroblast (MEF) feeder cells in knockout Dulbecco's modified Eagle's medium (Invitrogen) supplemented with 20% knockout serum replacement (KOSR), 1% nonessential amino acids, 2 mM L-glutamine (all from Invitrogen), 0.1 mM  $\beta$ -mercaptoethanol (Sigma) and 4 ng ml<sup>-1</sup> of basic fibroblast growth factor (bFGF; R&D systems).

**Differentiation through formation of embryoid bodies.** To induce the formation of embryoid bodies, undifferentiated hESCs were dissociated into small clumps with collagenase IV (Invitrogen) and transferred into non-adherent bacterial petri dishes containing hESC culture media (minus bFGF) supplemented with either FGF3 (50 ng ml<sup>-1</sup>) and FGF10 (250 ng ml<sup>-1</sup>) or EGF (20 ng ml<sup>-1</sup>) and IGF1 at (50 ng ml<sup>-1</sup>). This resulted in the formation of free-floating embryoid bodies. Cultures were maintained in a humidified chamber in a 5% CO<sub>2</sub> and air mixture at 37 °C. The embryoid bodies were cultured for 6 days and then allowed to attach onto tissue culture dishes coated with 0.1% gelatin. After 10 days, the cultures with EGF and IGF1 were supplemented with 10 ng ml<sup>-1</sup> bFGF for a further 6 to 8 days. FGF3 and FGF10 cells remained exposed to the growth factors throughout the experiment. All growth factors and supplements were obtained from R & D Systems or Invitrogen.

**Induction of otic progenitors directly as monolayers.** Undifferentiated hESCs were dissociated with 0.025% Trypsin-EDTA (Sigma) and the cell suspension passed through either a 70- or 100- $\mu$ m cell strainer (BD Labware). The 70- $\mu$ m strainer gave primarily a single-cell suspension, whereas the 100- $\mu$ m strainer retained a few 2-to-3-cell clumps. Cells were plated at different densities onto laminin-coated plastic (5  $\mu$ g cm<sup>-2</sup>; R&D systems.). Gelatin-coated dishes were also used, but the adhesion of cells proved to be very poor. Cells were incubated with chemically defined DFNB medium (DMEM high glucose: F12 mixed 1:1, with N2 and B27). This basal medium was supplemented, from the moment of plating, with either FGF3 (50 ng ml<sup>-1</sup>) and FGF10 (50 ng ml<sup>-1</sup>) and allowed to differentiate for 10 to 12 days or with EGF and IGF1 plus bFGF as described above for embryoid bodies formation. The medium was replaced completely every 2 days. During the first few days post plating, a high level of cell death is customary. **Colony enrichment and induction of differentiation into hair-cell-like cells and sensory neurons.** To enrich for OEPs, cells surrounding the epithelial colonies were lifted with a quick incubation in 0.025% Trypsin-EDTA, helped by mechanical scrapping under a microscope with a pipette tip. Once colonies edges started to curl (see Fig. 2c, d), cells were rinsed away. A second, prolonged trypsin step allowed the collection of epithelial colonies that remained attached.

To induce differentiation into hair-cell-like cells, we followed the protocol developed with hFASCs<sup>19</sup>. Dissociated cells were transferred to gelatin-coated dishes and cultured with DFNB supplemented with all-trans retinoic acid (10<sup>-6</sup> M; Sigma) and EGF (20 ng ml<sup>-1</sup>) for 2 to 4 weeks.

To enrich for ONPs, surrounding cells were scraped off under the microscope using a 10- $\mu$ l pipette tip bent at the end. Small colonies were then allowed to grow further for another 2 to 3 days, before being dissociated by trypsin. The use of these methods gave a fairly homogenous culture for the desired cell colony type.

To induce differentiation into auditory sensory neurons, dissociated cells were plated on gelatin-coated dishes and incubated in DFNB with bFGF (20 ng ml<sup>-1</sup>) and Sonic hedgehog (Shh-C24II, 500 ng ml<sup>-1</sup>; R&D Systems). On the third day, culture was supplemented with neurotrophin 3 (NTF3, 10 ng ml<sup>-1</sup>; Petropech) and brain-derived neurotrophic factor (BDNF, 10 ng ml<sup>-1</sup>; Petropech). Shh-C24II was removed on the fourth or fifth day, whereas the neurotrophins remained for the length of the incubation, normally between 7 and 14 days.

For proliferative expansion, progenitors were cultured in otic stem cell full media (OSCM; DFNB plus 20 ng ml<sup>-1</sup> bFGF, 50 ng ml<sup>-1</sup> IGF1 and 20 ng ml<sup>-1</sup> EGF).

**RNA isolation and gene expression analysis.** Total RNA was isolated using Trizol (Invitrogen) and was reverse transcribed into cDNA using Superscript III (Invitrogen). PCR was performed using standard protocols with Hotstar Taq polymerase (Qiagen).

Forward and reverse primer sequences, from the 5' to 3' direction, were as follows: PAX2, GAGCGAGTTCTCCGCAAC and GTCAGACGGGACGAT GTG; PAX8, ACCCCCAGGTGGTGGAGAAGA and CTCGAGGTGGTGCT GGCTGAAG; GAPDH, GTCCACTGGCGTCTCACCA and GTGGCAGTGA TGGCATGGAC; SOX2, ATGCACCGCTACGACGTGA and CTTTGACACC CCTCCCATTT; FGF3, TTGGAGATAACGGCAGTGG and CTCCAGGTTAT CGGGCTCT; PDS, AGCAGAGACAGGTCAATGAACC and AGATGGAA ACTGCAGCT; harmonin, AGCTGGTCATCAATGAACC and AGATGGAA TATCCATTGATCCG; POU4F3 (also known as BRN3C), TGCAAGAACCAAATTCTCC and GAGCTCTGGCTTGCTGTCT; GATA3, GTACAGCTCCGGACTCTCCCC and CTGCTCTCCTGGCTGCAGACA; MYO7A,

CACATCTTGCCATTGCTGAC and AGAAGAGAACCTCACAGGCAT; NEUROD1, GCCCCAGGGTTATGAGACTATCACT and CCGACAGAGC CCAGATGTAGTTCTT; ATOH1, CTCAGCCCCAGCTCTGC and AAAC AACGACCATCGCAGAG; HPRT, AATTATGGACAGGACTGAACGTC and CGTGGGGTCCTTTCACCAGCAAG; POU4F1 (also known as BRN3A), GGCCCACCTCAAGATCCCG and AGTTTCTCGCGATGGCGGC; NTRK2 (also known as TRKB), GAGCATCATGTACAGGAAAT and CTTGATGTT CTCTCTCATGT; ISLET1, CAACAAACAAAACGCAAAC and AAGTCAA ACACAATCCCGA.

Relative quantification of expression was performed using SYBR Green and the following primers: RPLPO, GAAGGCTGTGGTGTGATGG and CCGGAT ATGGAGGCAGCAGTT; PAX8, CTTGGCAGGTACTACGAGAC and GCAAC ATGGTAGGGTTCTG; PAX2, CTTAAAGAGATGTGCTGAGGG and CCT GTTCTGATTTGATGTGCT.  $\Delta$ Cts were calculated against the ribosomal protein RPLPO and  $\Delta\Delta$ Cts values compared against the levels expressed by undifferentiated hESCs. Undirected differentiation of embryoid bodies was induced by allowing the cells to aggregate in the presence of hES media (minus bFGF) supplemented with 5% FCS. Reactions were carried out in triplicate and values represent the mean from 2 to 4 independent experiments. Three different hESC lines were tested.

**Affymetrix microarrays.** Gene-expression profiles were obtained from hESC lines H14, Shef1 and Shef3 by hybridizing samples from undifferentiated, FGF3-and-FGF10-treated and DFNB-treated cells to Gene Chip HG-U133 Plus 2.0 arrays. Cells were cultured under differentiating conditions for 14 days before RNA was isolated. Normalization and initial analysis were done using puma (<http://www.bioconductor.org>). The chosen method is particularly robust and accurate when working with small sample sizes and the potentially high variability commonly found in human samples. Merging of the expression values from each experimental condition independently obtained from the three different cell lines was carried out using a hierarchical mixture of Gaussian distributions. The combined value for each transcript is the most probable value that represents the mixture of the two classes based on the uncertainty associated to each transcript at probe level. Analysis for the specific enrichment of otic markers was done using the Gene Set Enrichment Analysis (GSEA) tool<sup>24</sup>. This is a powerful algorithm that determines whether a set of genes is randomly distributed in a ranked list or primarily found at the top or bottom by calculating an enrichment score. This approach is based on the principle that a particular 'signature' of genes expressed together is highly informative, even if some individual genes change only by a small percentage (for example, 20%). This is because it identifies a structure of correlation within the genes rather than isolated outliers. A set of known pluripotency markers was run in parallel as a referential control. For the second analysis, probe sets were counted as differentially expressed if their expression changed by  $\geq$ 1.5-fold ( $\log_2$  0.5849) and their probability of positive log ratio (PPLR statistic) was  $>0.8$  for upregulated or  $<0.2$  for downregulated probe sets. Pathway and gene ontology (GO) enrichment analyses were carried out on these differentially expressed gene lists using the Database for Annotation, Visualization, and Integrated Discovery (DAVID; <http://david.abcc.ncifcrf.gov/home.jsp>). Functional annotation was used to reveal biological processes highly represented in a probe set list and the significance or likelihood of their enrichment expressed using the EASE score threshold (with  $P < 0.05$ ).

**Immunolabelling.** Cells and sections were fixed in cold 4% paraformaldehyde in PBS for 10 minutes, permeabilized and blocked in 0.1% Triton X-100, 5% normal donkey serum in PBS for 20 minutes at room temperature (20–25 °C) and then incubated with the primary antibody in the same buffer. Antibodies used in this study have been widely used and well characterized. These antibodies were against SOX2 (1:100, rabbit polyclonal, Millipore); nestin (1:100, mouse monoclonal, Abcam); PAX8 (1:100, goat polyclonal, Abcam); PAX2 (1:100, rabbit polyclonal, Abcam), GATA3 (1:50, mouse monoclonal, Santa Cruz), FOXG1 (1:50, rabbit polyclonal, Abcam), SIX1 (1:100, mouse monoclonal clone 3C7, Sigma), ATOH1 (1:100, rabbit polyclonal, Abcam); BRN3c (1:100, mouse polyclonal, Abnova), espin (1:100, rabbit polyclonal, Sigma);  $\beta$ -tubulin III (TUJ1) (1:100, mouse monoclonal, Covance); NF200 (1:100, rabbit polyclonal, Sigma), Synaptophysin (1:150, mouse monoclonal, Millipore), 3A10 (1:50, mouse monoclonal clone, DSHB, Iowa), BRN3a (1:100, rabbit polyclonal, Chemicon), NKA $\alpha$ 3 (1:75, goat polyclonal, Santa Cruz) and GluR2 (1:100, mouse monoclonal clone L21/32, Millipore). As GFP and tomato fluorescent protein can become downregulated after transplantation, their signal was amplified using either anti-GFP (1:100, rabbit polyclonal, Torrey Pines Biolabs) or anti-RFP (1:100, rabbit polyclonal, Abcam) antibodies. The myosin VIIA antibody was a gift from C. Petit. Specific labelling was visualized with secondary donkey anti-mouse, anti-goat or anti-rabbit antibodies conjugated to either Alexa Fluor 488 or Alexa Fluor 568. Controls were carried out by replacing the primary antibody with unspecific mouse or rabbit immunoglobulin-G (IgG). Nuclei were counterstained with DAPI (4',6-diamidino-2-phenylindole; Sigma).

Images were acquired using a Zeiss Axiophot microscope using Axio Vision software. For conventional quantification, several hundred cells were scored from random fields from two to five independent experiments. Statistical comparisons of means were made using analysis of variance (ANOVA; two-way ANOVA followed by the Bonferroni post test). For all statistical tests  $P < 0.05$  was used as the criterion for statistical significance.

**Quantification using the InCell Analyzer.** The hESC lines H7, H14 and Shef3 were seeded at 1,500 cells per well of a 96-well clear flat-bottom plate (655090; Greiner Bio-one) in either FGF or DFNB media. Images of several thousand stained cells from three independent wells were acquired using an automated microscopy platform (InCell Analyzer 1000, GE Healthcare). Forty random fields were acquired in each well using a  $\times 20$  objective. Images were analysed using Developer Toolbox 1.7 software (GE Healthcare).

Nuclei were counted as positive at two different thresholds of fluorescent intensity; these were set independently for each cell line and plate. The first threshold was set according to the fluorescent intensity distribution histogram of the cells in the control (no primary antibody) wells: cells were counted as positive, green or red, if the nuclei intensity was greater than the 99th intensity percentile point in channel 2 (green) or 3 (red), respectively. Similarly, a second threshold was set to count very highly positive cells. This was determined from the fluorescent intensity distribution of the cells grown in FGF; cells were counted as highly positive if the nuclei intensity was greater than the 75th intensity percentile point in this condition. Significance was determined using Chi-square with Yates' correction.

**Electrophysiology.** Membrane currents from undifferentiated cells, and differentiating hair-cell-like cells and sensory neurons were measured using the whole-cell patch-clamp technique with an Optopatch (Cairn Research) or axopatch 200B (Molecular Devices) amplifiers. Recordings were carried out at room temperature ( $20\text{--}25^\circ\text{C}$ ) from cells cultured between 9 and 19 days under either 'hair cell' or 'neuralizing' conditions, or soon after completing the induction with FGF3 and FGF10 (undifferentiated). Current clamp recordings of neuron-like cell-voltage responses were performed at body temperature ( $35\text{--}37^\circ\text{C}$ ). The extracellular solution contained (in mM): 135 NaCl, 5.8 KCl, 1.3 CaCl<sub>2</sub>, 0.9 MgCl<sub>2</sub>, 0.7 NaH<sub>2</sub>PO<sub>4</sub>, 5.6 D-glucose, 10 HEPES-NaOH and 2 sodium pyruvate. Amino acids and vitamins for Eagle's minimal essential medium (MEM) were added from concentrates (Fisher). The pH was adjusted to 7.5. Cells were viewed using an upright microscope (Leica) and continuously superfused with the above extracellular solution. Patch pipettes were made from soda glass capillaries (3–4 MΩ) and coated with surf wax. The pipette filling solution contained (in mM): 131 KCl, 3 MgCl<sub>2</sub>, 1 EGTA-KOH, 5 Na<sub>2</sub>ATP, 5 Hepes-KOH and 10 sodium phosphocreatine (pH 7.3).

Data were acquired using pClamp software and a Digidata analogue-to-digital converter (Molecular Devices). Data were filtered at 2.5 or 5 kHz, sampled at 5 or 50 kHz and stored on computer for off-line analysis using Clampfit and Origin (OriginLab) software. Membrane capacitance ( $C_m$ ) was  $30 \pm 4$  pF ( $n = 43$ , range from 9 to  $>100$  pF) and residual series resistance was  $7.8 \pm 0.7$  MΩ, resulting in voltage-clamp time constants of  $244 \pm 40$  μs. Membrane currents were elicited by applying voltage steps in 10-mV nominal increments or decrements from the holding potential of -84 mV or -104 mV (for  $I_{\text{K}}$ ,  $I_{\text{Ca}}$  and  $I_{\text{Na}}$ ) or -64 mV (for  $I_{\text{K1}}$ ).

Recordings and reported currents were corrected off-line for linear leakage, typically calculated between -84 mV and -74 mV (undifferentiated cells:  $0.4 \pm 0.1$  ns,  $n = 6$ ; hair-cell-like cells:  $2.3 \pm 0.8$  ns,  $n = 14$ , neuron-like cells:  $1.7 \pm 0.6$  ns,  $n = 15$ ). Membrane potentials were corrected for the voltage drop across the residual series resistance ( $R_s$ ) and for a liquid junction potential of -4 mV. Statistical comparisons of means were made using ANOVA (one-way ANOVA followed by the Tukey post-test). For all statistical tests  $P < 0.05$  was used as the criterion for statistical significance. Mean values are quoted  $\pm$  s.e.m. in text and figures.

**Transplantation and cochleae processing.** Animal experiments were approved by the Sheffield University Ethical Review Committee and carried out under a Home Office Project License conforming to UK legislation. Anaesthesia in young, adult gerbils (3–8 months old) was induced with ketamine and xylazine, and maintained with isoflurane during the surgical intervention. Before the deafening procedure, auditory function was measured as described below. Under sterile conditions and using a retro-auricular approach, the bulla from the left ear was exposed and a small hole opened on its surface. Twenty microlitres of a 1-mM ouabain solution (Sigma) were applied to the round-window niche, incubated for 30 min and then absorbed with a small cotton wick. The right cochlea was left undisturbed and used as a control in each animal. Opening in the bulla was sealed

with a bit of fascia and Vetbond (3M), the surgical wound closed with sutures and the animal allowed to recover for 3 days.

Before cell transplantation, auditory function was measured to ascertain the efficacy of the deafening protocol. Bulla was exposed as before and the round-window niche re-opened. A small hole was drilled into the modiolus by going through the round-window membrane, using a 30G needle or a KFlex dental file (no. 25). Human ONPs, expanded in OSCFM, were dissociated and collected to a density of  $1.5 \times 10^4$  cells per  $\mu\text{l}$  in DMEM. About 3  $\mu\text{l}$  ( $4\text{--}5 \times 10^4$  cells) were injected into the central modiolus using a stainless steel NanoFil syringe (WPI) with a 33G tungsten bevelled needle. Control animals underwent an identical intervention, but were transplanted with DMEM only. To prevent rejection, gerbils were given daily injections of cyclosporine A ( $15 \text{ mg kg}^{-1} \text{ day}^{-1}$ ; Sandoz).

At selected time points, animals were killed and fixed by transcardiac perfusion with 4% paraformaldehyde in PBS. Cochleae were removed, post-fixed overnight and decalcified by immersion in 0.125 M EDTA for approximately 2 weeks. Tissue was embedded in Cryo-M-Bed (Bright) and sectioned in a cryostat.

**Spiral ganglion cell densities.** Cells present after ouabain treatment and after transplantation, and expressing the appropriated markers were counted in the apical, mid and basal turns in 7 to 27 randomly selected mid-modiolus sections from each cochlea. The area was measured using ImageJ and densities calculated as cells per mm<sup>2</sup>. Statistical comparisons of means were made using ANOVA. For all statistical tests  $P < 0.05$  was used as the criterion for statistical significance. Mean values are quoted  $\pm$  s.e.m. in text and figures.

**ABRs and DPOAEs.** ABR testing was conducted in an isolated laboratory room. Prior to testing, the gerbils were sedated with ketamine and xylazine and placed on a heating pad. The ABRs were recorded using System 3 digital signal processing hardware and software (Tucker Davis Technologies (TDT)). ABR stimuli were presented using two enhanced real-time processors (RP2.1), a programmable attenuator (PA-5) to control the stimulus levels and closed-field magnetic speakers (CF1). The CF1 speaker presented the ABR stimuli through a 10-cm tube that allowed its delivery directly into the ear canal. The ABR responses were recorded using 27GA subdermal needle electrodes (Rochester Electro-Medical) connected to a low impedance headstage (RA4LI) and medusa preamplifier (RA4PA) before sending them to a medusa base station signal processor (RA16). Click stimuli were presented at a rate of  $20 \text{ s}^{-1}$ , ranging from 80 dB SPL to 20 dB SPL in 10-dB decrements. For tone ABRs, 5-ms pure-tone pips (ranging from 6 kHz to 38 kHz in 4-kHz increments) were presented at an intensity of 80 dB SPL. The ABR waveforms were produced through differential voltage recordings from electrodes placed at the vertex (recording electrode) and ipsilateral mastoid (reference electrode), with the ground electrode placed on the lower back. Each ABR waveform represented the average response to 500 stimulus presentations. The amplitude between the wave ii positive peak and wave iii negative peak were measured for each dB SPL, and the ABR thresholds were determined as the stimulus level that evoked a voltage that was 2 s.d. above the mean background noise level.

DPOAE testing was conducted in the same room, and gerbils were prepared for the procedure as they were for ABRs testing. DPOAEs were recorded using the same TDT workstation under different settings. The instrumentation used to present the DPOAE stimuli consisted of a single ear probe unit to direct the stimuli into the ear canal by the Etymotic ER-10B<sup>®</sup> low noise microphone system that provided 20 dB of gain, and a microphone amplifier (MA-3) that provided an additional 20 dB of gain to the DPOAE responses prior to digital conversion. The sampling rates to generate stimuli and digitize the responses were 100 kHz. The DPOAEs were generated by simultaneously presenting two sinusoids differing in frequency into the ear canal of the gerbil (the lower frequency was labelled f1 and the higher frequency was labelled f2). The amplitude of the distortion product at the frequency defined by  $2f_1 - f_2$  was then measured by recording the pressure in the ear canal. The stimuli were selected for DPOAE testing from 6 kHz to 42 kHz with 4-kHz increments. The sound levels for the f1 and f2 primaries were calibrated to 65 dB SPL and 60 dB SPL, respectively, using an ACOustical interface system (ACO Pacific) with a 2-cm calibration syringe.

All ABR and DPOAE stimuli were created using TDT SigGen and recordings conducted using TDT BioSig software. Statistical comparisons of means were made using either the unpaired Student's two-tailed *t*-test for two data sets, or for comparisons of multiple data sets, using ANOVA (two-way ANOVA followed by the Bonferroni post test). For all statistical tests  $P < 0.05$  was used as the criterion for statistical significance. Mean values are quoted  $\pm$  s.e.m. in text and figures.